Design and Implementation of a Hard Disk Drive Servo System Using Robust and Perfect Tracking Approach

Teck B. Goh, Zhongming Li, Ben M. Chen, *Member, IEEE*, Tong Heng Lee, and Tony Huang, *Member, IEEE*

***Abstract*—This paper deals with the problem of a servo system design for a conventional hard disk drive with a single voice-coil-motor (VCM) actuator using a so-called robust and perfect tracking (RPT) approach. We will first model the physical system and then formulate it into a robust and perfect tracking problem, in which a measurement feedback controller can be obtained to achieve a robust and perfect tracking for any step reference, i.e., the L_p-norm of the resulting tracking error with $1 \leq p < \infty$ can be made arbitrarily small in the presence of external disturbances and initial conditions. Some tradeoffs are then made in order for the RPT controller to be implementable using the existing hardware setup. The implementation results of the RPT controller are compared with those of a proportional integral derivative (PID) controller. The results show that the servo system with our RPT controller has much better performance than the PID one has. Our servo system has faster settling time, lower overshoot and higher accuracy.**

***Index Terms*—Actuators, modeling, perfect tracking, robust control, servo systems.**

I. Introduction

HARD disk drives provide important data-storage medium for computers and other data-processing systems. In most hard disk drives, rotating disks coated with a thin magnetic layer or recording medium are written with data, which are arranged in concentric circles or tracks. Data are read or written with a read/write (R/W) head, which consists of a small horseshoe-shaped electromagnet. Fig. 1 shows a simple illustration of a typical hard disk servo system.

The two main functions of the R/W head positioning servo mechanism in disk drives are track seeking and track following. Track seeking moves the R/W head from the present track to a specified destination track in minimum time using a bounded control effort. Track following maintains the head as close as possible to the destination track center while information is being read from or written to the disk. Track density is the reciprocal of the track width. It is suggested that on a disk surface, tracks should be written as closely spaced as possible so that we can maximize the usage of the disk surface. This means an increase in the track density, which subsequently means a more stringent requirement on the allowable variations of the position of the heads from the true track center.

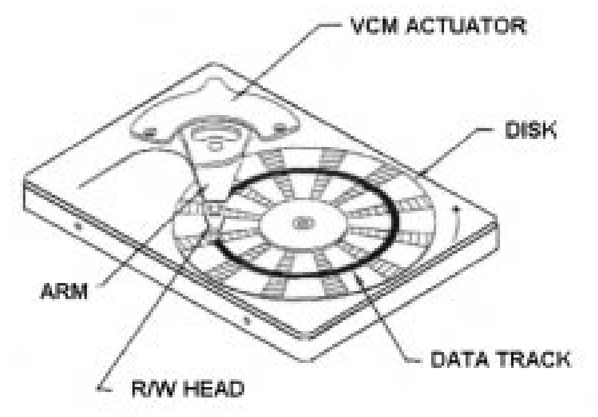

Fig. 1. A hard disk drive with a VCM actuator servo system.

The prevalent trend in hard disk design is toward smaller hard disks with increasingly larger capacities. This implies that the track width has to be smaller leading to lower error tolerance in the positioning of the head. The controller for track following has to achieve tighter regulation in the control of the servomechanism. Current hard disk drives use a combination of classical control techniques, such as lead-lag compensators, PI compensators, and notch filters. These classical methods can no longer meet the demand for hard disk drives of higher performance. So many control approaches have been tried, such as linear quadratic Gaussian (LQG) and/or LTR approach (see, e.g., [8] and [16]), H_∞ almost disturbance decoupling approach (see, e.g., [4]), and adaptive control (see, e.g., [11]) and so on. Although much work has been done to date, more studies need to be conducted to use more control methods to achieve better performance of the hard disk drives.

The purpose of this project is to use the newly developed robust and perfect tracking (RPT) control method in the hard disk drive servo system. This paper focuses on the modeling and control design of the voice coil motor (VCM) actuator for hard disk R/W heads. We will first obtain a model of the VCM actuator and then cast the overall servo system design into an RPT design framework. A first-order dynamic measurement feedback controller is then designed to achieve a robust and perfect tracking for any step reference. Our controller is theoretically capable of making the L_p-norm of the resulting tracking error

Manuscript received March 18, 1999. Recommended by Associate Editor D. W. Repperger.

T. B. Goh, Z. Li, and B. M. Chen are with the Department of Electrical Engineering, the National University of Singapore, Singapore 117576. They are also with the Data Storage Institute, Singapore 117608.

T. H. Lee is with the Department of Electrical Engineering, the National University of Singapore, Singapore 117576.

T. Huang is with the Data Storage Institute, Singapore 117608.

Publisher Item Identifier S 1063-6536(01)00522-X.

with $1 \leq p < \infty$ arbitrarily small in faces of external disturbances and initial conditions. Some tradeoffs are then made in order for the RPT controller to be implementable using the existing hardware setup and to meet physical constraints such as sampling rates and the limit of control of the system. The implementation results of the RPT controller are compared with those of a PID controller. The results show that our servo system is simpler and yet has faster seeking times, lower overshoot and higher accuracy.

The outline of this paper is as follows: in the next section, we identify a fourth-order model for the VCM actuator of a typical hard disk drive. The model is obtained using a frequency response identification method. In Section III, we cast our servo design problem into a robust and perfect tracking control framework to obtain a family of first-order measurement feedback controllers. It is parameterized by a tuning parameter ε, which can be tuned such that the overall design meets desired design specifications. The experimental results of the RPT control system are given in Section IV with a detailed comparison with the results of a PID controller. Finally, the concluding remarks and comments are drawn in Section V.

II. Modeling of the VCM Actuator

In this section, we present the modeling of the VCM actuator, which is well known in the research community of the hard disk drive servo systems to have a characteristic of a double integrator cast with some high frequency resonance, which can reduce the system stability if neglected. There are some bias forces in the hard disk drive system which will cause steady-state error in tracking performance. Moreover, there are also some nonlinearities in the system at low frequencies, which are primarily due to the pivot and bearing frictions. All these factors should be taken into consideration when considering the design of a controller for the VCM. For the purpose of developing a model, we have to compromise between accuracy and simplicity. In this section, a relatively simplified model of the VCM is identified and presented.

We utilize the frequency response identification method (see, e.g., [5] and [14]) to model our actuator. Such a method is applicable to minimum phase processes. We expect from the properties of the physical system that the VCM actuator should be of minimum phase. Thus, the method of [5] can be employed to identify our VCM model.

The dynamics of an ideal VCM actuator can be formulated as a second-order state-space model as the following (see, e.g., [15]),

$$\begin{pmatrix} \dot{y} \\ \dot{v} \end{pmatrix} = \begin{pmatrix} 0 & k_y \\ 0 & 0 \end{pmatrix} \begin{pmatrix} y \\ v \end{pmatrix} + \begin{pmatrix} 0 \\ k_v \end{pmatrix} u \tag{1}$$

where

u	actuator input (in volts);
y and v	position (in tracks) and the velocity of the R/W head;
k_y	position measurement gain;
k_t	current-force conversion coefficient;
m	mass of the VCM actuator;
k_v	$= k_t/m$

Thus, the transfer function of an ideal VCM model appears to be a double integrator, i.e.,

$$G_{v1}(s) = \frac{k_v k_y}{s^2}. \tag{2}$$

However, if we consider also the high-frequency resonance modes, a more realistic model for the VCM actuator should be

$$G_v(s) = \frac{k_v k_y}{s^2} \frac{k_d s + \omega_n^2}{s^2 + 2\xi\omega_n s + \omega_n^2}. \tag{3}$$

Using the algorithm of [5] and the measured data from the actual system (see Fig. 2), we obtain a fourth-order model for the actuator

$$G_v(s) = \frac{4.3817 \times 10^{10} s + 4.3247 \times 10^{15}}{s^2(s^2 + 1.5962 \times 10^3 s + 9.7631 \times 10^7)}. \tag{4}$$

Fig. 2 shows that the frequency response of the identified model matches the measured data very well for the frequency range from 0–10^4 rad/s, which far exceeds the working range of the VCM actuator.

III. Control System Design Using the RPT Approach

We now present the servo system design for the actuator identified in the previous section. Basically, almost all commercially available hard disk drive servo systems up-to-date are designed using conventional PID approach. For drives with a single VCM actuator, designers would encounter problems if they wish to push up the tracking following speed. Usually, there will be some huge peak overshoot in step response. Thus, in practice, one would have to make tradeoffs between the track following speed and overshoot by selecting appropriate PID controller gains. We introduce in this section the so-called robust and perfect tracking (RPT) control technique. Such an approach will enable the designer to design a very low-order control law, and moreover, the resulting closed-loop system will have fast track following speed and low overshoot as well as strong robustness. For the benefits of general readers, we recall briefly the theory and design procedure of the RPT approach without detailed proofs.

We consider a general linear system with external disturbances described by the following state-space model Σ:

$$\left.\begin{aligned} \dot{x} &= Ax + Bu + Ew, \qquad x(0) = x_0 \\ y &= C_1 x + D_1 w \\ h &= C_2 x + D_2 u \end{aligned}\right\} \tag{5}$$

where

$x \in \mathbb{R}^n$	state variable of the system;
$u \in \mathbb{R}^m$	control;
$w \in \mathbb{R}^k$	external disturbance;
$y \in \mathbb{R}^q$	measurement output;
$h \in \mathbb{R}^\ell$	output to be controlled.

For simplicity, we will only consider a step reference signal $r(t) \in \mathbb{R}^\ell$ in this paper. Then the robust and perfect tracking

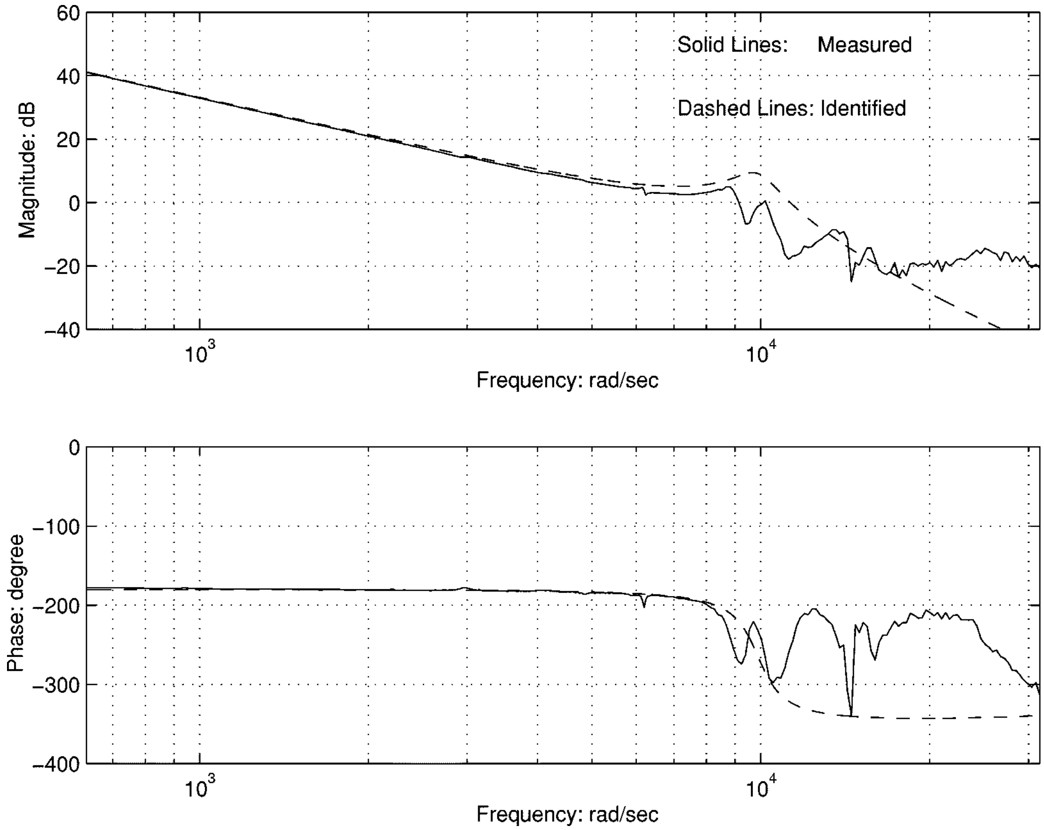

Fig. 2. Frequency responses of the actual and identified models of the VCM actuator.

(RPT) problem is to design a parameterized controller of the following form $\sum_v(\varepsilon)$:

$$\left.\begin{aligned}\dot{x}_v &= A_{vv}(\varepsilon)x_v + B_{vy}(\varepsilon)y + B_{vr}(\varepsilon)r \\ u &= C_{vv}(\varepsilon)x_v + D_{vy}(\varepsilon)y + D_{vr}(\varepsilon)r\end{aligned}\right\} \tag{6}$$

where $x_v \in \mathbb{R}^{n_v}$ is the state variable of the control law, such that the following properties hold.

1) The resulting closed-loop system comprising the system Σ of (5) and the control law $\Sigma_v(\varepsilon)$ of (6) is internally stable for all $\varepsilon \in (0, \varepsilon^\star]$, where $\varepsilon^\star$ is a positive scalar.
2) Let $e = h - r$. For any $w \in L_p$, $p \in [1, \infty)$, and any initial condition x_0, the resulting tracking error satisfies

$$\|e\|_p \to 0, \quad \text{as } \varepsilon \to 0. \tag{7}$$

Obviously, e is a function of ε. The above property implies that h is capable of tracking r with arbitrarily fast settling time in faces of external disturbances and initial conditions.

It is shown in [10] that the above RPT problem is solvable if and only if the following conditions are satisfied:

1) (A, B) is stabilizable and (A, C_1) is detectable;
2) (A, B, C_2, D_2) is minimum phase and right invertible;
3) $\text{Ker}(C_2) \supseteq C_1^{-1}\{\text{Im}(D_1)\} := \{v | C_1 v \in \text{Im}(D_1)\}$.

By minimum phase we mean that (A, B, C_2, D_2) does not have invariant zeros in the closed right-half complex plane. Note that for the case when $D_1 = 0$, item 3 above is equivalent to $\text{Ker}(C_2) \supseteq \text{Ker}(C_1)$. In what follows, we will give an algorithm that constructs a reduced order measurement feedback control law to solve the RPT problem under the above necessary and sufficient conditions. Let

$$r(t) = \begin{bmatrix}\alpha_1 \\ \alpha_2 \\ \vdots \\ \alpha_\ell\end{bmatrix} \cdot 1(t) = \boldsymbol{\alpha} \cdot 1(t) \tag{8}$$

where $1(t)$ is the unit step function, and $\alpha_1, \alpha_2, \ldots, \alpha_\ell$ are the magnitudes of the step functions. Thus, we have

$$\dot{r}(t) = \boldsymbol{\alpha} \cdot \delta(t) \tag{9}$$

where $\delta(t)$ is a unit impulse function. Then, we obtain an auxiliary system $\sum_{aux}$, which combines the original system $\sum$ of (5) and the reference signal $r(t)$, as the following:

$$\left.\begin{aligned}\dot{\boldsymbol{x}} &= \boldsymbol{A}\boldsymbol{x} + \boldsymbol{B}u + \boldsymbol{E}\boldsymbol{w} \\ \boldsymbol{y} &= \boldsymbol{C}_1\boldsymbol{x} + \boldsymbol{D}_1\boldsymbol{w} \\ e &= \boldsymbol{C}_2\boldsymbol{x} + \boldsymbol{D}_2 u\end{aligned}\right\} \tag{10}$$

where

$$\boldsymbol{x} = \begin{pmatrix} r \\ x \end{pmatrix}, \ \boldsymbol{w} = \begin{pmatrix} w \\ \boldsymbol{\alpha}\delta(t) \end{pmatrix}, \ \boldsymbol{y} = \begin{pmatrix} r \\ y \end{pmatrix} \tag{11}$$

and

$$\boldsymbol{A} = \begin{bmatrix} 0 & 0 \\ 0 & A \end{bmatrix}, \ \boldsymbol{B} = \begin{bmatrix} 0 \\ B \end{bmatrix}, \ \boldsymbol{E} = \begin{bmatrix} 0 & I_\ell \\ E & 0 \end{bmatrix} \tag{12}$$

$$\boldsymbol{C}_2 = [-I \quad C_2], \ \boldsymbol{D}_2 = D_2 \tag{13}$$

$$\boldsymbol{C}_1 = \begin{bmatrix} I & 0 \\ 0 & C_1 \end{bmatrix}, \ \boldsymbol{D}_1 = \begin{bmatrix} 0 & 0 \\ D_1 & 0 \end{bmatrix}. \tag{14}$$

It can be easily shown that the quadruple $(\boldsymbol{A}, \boldsymbol{B}, \boldsymbol{C}_2, \boldsymbol{D}_2)$ has the same infinite zero structure and the same stable invariant zeros as those of (A, B, C_2, D_2), and is right invertible as well but with ℓ additional invariant zeros at the origin. The construction algorithm involves two step main stages: In the first stage, we will construct a static state feedback law for $\sum_{aux}$ of (10) which will solve the RPT problem for the case when $y = x$, i.e., all the states of $\sum$ are available for measurement. Then, in the second stage, we design a reduced order measurement feedback control law that will recover the performance of the static state feedback law designed in the first stage. The following algorithm is due to [10]:

Stage 1: The following stage is to construct a parameterized state feedback gain $\boldsymbol{F}(\varepsilon)$ such that $\boldsymbol{u} = \boldsymbol{F}(\varepsilon)\boldsymbol{x}$ will solve the RPT problem for the system of (5) with $C_1 = I$ and $D_1 = 0$, i.e., its corresponding auxiliary system of (10) can be rewritten as

$$\left.\begin{aligned} \dot{\boldsymbol{x}} &= \boldsymbol{A}\boldsymbol{x} + \boldsymbol{B}u + \boldsymbol{E}\boldsymbol{w} \\ \boldsymbol{y} &= \boldsymbol{x} \\ e &= \boldsymbol{C}_2\boldsymbol{x} + \boldsymbol{D}_2 u \end{aligned}\right\}. \tag{15}$$

Note that $(\boldsymbol{A}, \boldsymbol{B}, \boldsymbol{C}_2, \boldsymbol{D}_2)$ is right invertible and has invariable zeros at the origin.

Step S.F.1: Utilize the results of the special coordinate basis of [13] and [12] (see also [1] for the detailed proofs of its properties) to find nonsingular state, input, and output transformations Γ_s, Γ_i and Γ_o to the system (15) such that if we let

$$\boldsymbol{x} = \Gamma_s\tilde{x},\ e = \Gamma_o\tilde{e},\ u = \Gamma_i\tilde{u} \tag{16}$$

we will have

$$\tilde{x} = \begin{pmatrix} x_a^0 \\ x_a^- \\ x_c \\ x_d \end{pmatrix},\ x_d = \begin{pmatrix} x_1 \\ x_2 \\ \vdots \\ x_{m_d} \end{pmatrix},\ \tilde{e} = \begin{pmatrix} e_0 \\ e_d \end{pmatrix}, \tag{17}$$

$$e_d = \begin{pmatrix} e_1 \\ e_2 \\ \vdots \\ e_{m_d} \end{pmatrix},\ \tilde{u} = \begin{pmatrix} u_0 \\ u_d \\ u_c \end{pmatrix},\ u_d = \begin{pmatrix} u_1 \\ u_2 \\ \vdots \\ u_{m_d} \end{pmatrix} \tag{18}$$

and

$$\dot{x}_a^0 = A_{aa}^0 x_a^0 + B_{0a}^0 e_0 + L_{ad}^0 e_d + E_a^0 \boldsymbol{w} \tag{19}$$

$$\dot{x}_a^- = A_{aa}^- x_a^- + B_{0a}^- e_0 + L_{ad}^- e_d + E_a^- \boldsymbol{w} \tag{20}$$

$$\begin{aligned} \dot{x}_c &= A_{cc}x_c + B_c E_{ca}^0 x_a^0 + B_c E_{ca}^- x_a^- \\ &\quad + B_{0c}e_0 + L_{cd}e_d + B_c u_c + E_c\boldsymbol{w} \end{aligned} \tag{21}$$

$$e_0 = C_{0a}^0 x_a^0 + C_{0a}^- x_a^- + C_{0c}x_c + C_{0d}x_d + u_0 \tag{22}$$

and for each $i = 1, \ldots, m_d$

$$\begin{aligned} \dot{x}_i &= A_{q_i}x_i + L_{i0}e_0 + L_{id}e_d + E_{di}w + B_{q_i} \\ &\quad \cdot \left[u_i + E_{ia}^0 x_a^0 + E_{ia}^- x_a^- + E_{ic}x_c + \sum_{j=1}^{m_d} E_{ij}x_j\right] \end{aligned} \tag{23}$$

$$e_i = C_{q_i}x_i, \quad e_d = C_d x_d. \tag{24}$$

Here the states x_a^0, x_a^-, x_c and x_d are, respectively, of dimensions n_a^0, n_a^-, n_c and $n_d = \sum_{i=1}^{m_d} q_i$, while x_i is of dimension q_i for each $i = 1, \ldots, m_d$. The control vectors u_0, u_d and u_c are, respectively, of dimensions $m_0 = \text{rank}(D_2)$, m_d and $m_c = m - m_0 - m_d$ while the output vectors e_0 and e_d are, respectively, of dimensions $p_0 = m_0$ and $p_d = m_d$. The matrices A_{q_i}, B_{q_i} and C_{q_i} have the following form:

$$A_{q_i} = \begin{bmatrix} 0 & I_{q_i-1} \\ 0 & 0 \end{bmatrix},\ B_{q_i} = \begin{bmatrix} 0 \\ 1 \end{bmatrix} \tag{25}$$

and

$$C_{q_i} = [1 \quad 0 \quad \ldots \quad 0]. \tag{26}$$

Moreover, the eigenvalues of A_{aa}^0 are all at the origin, the eigenvalues of A_{aa}^- are all in the left half complex plane, i.e., they are stable, and the pair (A_{cc}, B_c) is controllable.

Step S.F.2: Let F_c be any arbitrary $m_c \times n_c$ matrix subject to the constraint that

$$A_{cc}^c = A_{cc} - B_c F_c \tag{27}$$

is a stable matrix.

Step S.F.3: This step deals with the infinite zero structure of the given system, i.e., subsystems, $i = 1$ to m_d, represented by (23). Let $\Lambda_i = \{\lambda_{i1}, \lambda_{i2}, \ldots, \lambda_{iq_i}\}$, $i = 1$ to m_d, be the sets of q_i elements all in $\mathbb{C}^-$, which are closed under complex conjugation. Next, we let $\Lambda_d := \Lambda_1 \cup \Lambda_2 \cup \ldots \cup \Lambda_{m_d}$. For $i = 1$ to m_d, define

$$\begin{aligned} p_i(s) &:= \prod_{j=1}^{q_i}(s - \lambda_{ij}) \\ &= s^{q_i} + F_{i1}s^{q_i-1} + \ldots + F_{iq_i-1}s + F_{iq_i} \end{aligned}$$

and

$$\tilde{F}_i(\varepsilon) := \frac{1}{\varepsilon^{q_i}} F_i S_i(\varepsilon) \tag{28}$$

where

$$F_i = [F_{iq_i} \quad F_{iq_i-1} \quad \ldots \quad F_{i1}] \tag{29}$$

and

$$S_i(\varepsilon) = \text{diag}\{1, \varepsilon, \varepsilon^2, \ldots, \varepsilon^{q_i-1}\}. \tag{30}$$

Step S.F.4: The parameterized gain matrix is given by

$$\boldsymbol{F}(\varepsilon) := -\Gamma_i \begin{bmatrix} C_{0a}^0 & C_{0a}^- & C_{0c} & C_{0d} \\ E_{da}^0 & E_{da}^- & E_{dc} & \tilde{F}_d(\varepsilon) + E_d \\ E_{ca}^0 & E_{ca}^- & F_c & 0 \end{bmatrix} \Gamma_s^{-1} \tag{31}$$

where

$$E_{da}^0 = \text{diag}\{E_{1a}^0, \ldots, E_{m_d a}^0\} \tag{32}$$

$$E_{da}^- = \text{diag}\{E_{1a}^-, \ldots, E_{m_d a}^-\} \tag{33}$$

$$E_{dc} = \text{diag}\{E_{1c}, \ldots, E_{m_d c}\} \tag{34}$$

$$\tilde{F}_d(\varepsilon) = \mathrm{diag}\left\{\tilde{F}_1(\varepsilon),\, \tilde{F}_2(\varepsilon),\, \ldots,\, \tilde{F}_{m_d}(\varepsilon)\right\} \tag{35}$$

and

$$E_d = \begin{bmatrix} E_{11} & \cdots & E_{1m_d} \\ \vdots & \ddots & \vdots \\ E_{m_d1} & \cdots & E_{m_dm_d} \end{bmatrix}. \tag{36}$$

Finally, we partition

$$\boldsymbol{F}(\varepsilon) = [\, H(\varepsilon) \quad F(\varepsilon)\,] \tag{37}$$

where $H(\varepsilon) \in \mathbb{R}^{m\times\ell}$ and $F(\varepsilon) \in \mathbb{R}^{m\times n}$.

Stage 2: We now design a reduced order measurement feedback controller that solves the RPT problem for the system (5). For simplicity of presentation, we assume that matrices C_1 and D_1 have already been transformed into the following forms:

$$C_1 = \begin{bmatrix} 0 & C_{1,02} \\ I_k & 0 \end{bmatrix} \text{ and } D_1 = \begin{bmatrix} D_{1,0} \\ 0 \end{bmatrix} \tag{38}$$

where $D_{1,0}$ is of full row rank. We first partition the following system:

$$\left.\begin{aligned} \dot{x} &= Ax + Bu + [\,E \quad I_n\,]\tilde{w}, \\ y &= C_1x + [\,D_1 \quad 0\,]\tilde{w}, \end{aligned}\right\} \tag{39}$$

in conformity with the structures of C_1 and D_1 in (38), i.e.,

$$\left.\begin{aligned} \begin{pmatrix} \dot{x}_1 \\ \dot{x}_2 \end{pmatrix} &= \begin{bmatrix} A_{11} & A_{12} \\ A_{21} & A_{22} \end{bmatrix}\begin{pmatrix} x_1 \\ x_2 \end{pmatrix} + \begin{bmatrix} E_1 & I_k & 0 \\ E_2 & 0 & I_{n-k} \end{bmatrix}\tilde{w} \\ &\quad + \begin{bmatrix} B_1 \\ B_2 \end{bmatrix} u \\ \begin{pmatrix} y_0 \\ y_1 \end{pmatrix} &= \begin{bmatrix} 0 & C_{1,02} \\ I_k & 0 \end{bmatrix}\begin{pmatrix} x_1 \\ x_2 \end{pmatrix} + \begin{bmatrix} D_{1,0} & 0 & 0 \\ 0 & 0 & 0 \end{bmatrix}\tilde{w} \end{aligned}\right\} \tag{40}$$

where

$$\tilde{w} = \begin{pmatrix} w \\ x_0 \cdot \delta(t) \end{pmatrix}. \tag{41}$$

Obviously, $y_1 = x_1$ is directly available and hence need not to be estimated. Next, we define $\sum_{QR}$ to be characterized by $(A_R,\, E_R,\, C_R,\, D_R)$ with

$$A_R = A_{22},\, E_R = [\,E_2 \quad 0 \quad I_{n-k}\,] \tag{42}$$

and

$$C_R = \begin{bmatrix} C_{1,02} \\ A_{12} \end{bmatrix},\, D_R = \begin{bmatrix} D_{1,0} & 0 & 0 \\ E_1 & I_k & 0 \end{bmatrix}. \tag{43}$$

It is again straightforward to verify that $\sum_{QR}$ is right invertible with no finite and infinite zeros. Moreover, $(A_R,\, C_R)$ is detectable if and only if $(A,\, C_1)$ is detectable. We also partition $F(\varepsilon)$ of (37) in conformity with x_1 and x_2 as follows:

$$F(\varepsilon) = [\,F_1(\varepsilon) \quad F_2(\varepsilon)\,]. \tag{44}$$

Next, let K_R be an appropriate dimensional constant matrix such that the eigenvalues of

$$A_R + K_RC_R = A_{22} + [\,K_{R0} \quad K_{R1}\,]\begin{bmatrix} C_{1,02} \\ A_{12} \end{bmatrix} \tag{45}$$

are all in $\mathbb{C}^-$. This can be done because $(A_R,\, C_R)$ is detectable. Then, the reduced order measurement feedback law that solves the RPT problem is given by (6) with

$$\left.\begin{aligned} A_{vv}(\varepsilon) &= A_R + B_2F_2(\varepsilon) + K_RC_R + K_{R1}B_1F_2(\varepsilon) \\ B_{vy}(\varepsilon) &= G_R(\varepsilon) + (B_2 + K_{R1}B_1)[0,\, F_1(\varepsilon) - F_2(\varepsilon)K_{R1}] \\ B_{vr}(\varepsilon) &= (B_2 + K_{R1}B_1)H(\varepsilon) \\ C_{vv}(\varepsilon) &= F_2(\varepsilon) \\ D_{vy}(\varepsilon) &= [0,\, F_1(\varepsilon) - F_2(\varepsilon)K_{R1}] \\ D_{vr}(\varepsilon) &= H(\varepsilon) \end{aligned}\right\} \tag{46}$$

where

$$G_R(\varepsilon) = [-K_{R0},\, A_{21} + K_{R1}A_{11} - (A_R + K_RC_R)K_{R1}].$$

We note that there are software packages available (see, e.g., [2] and [9]) to construct the special coordinate basis of linear systems and the above algorithm for realizing the RPT controllers. The following theorem is due to [10].

Theorem 1: Consider the system $\sum$ of (5), which satisfies all the three conditions for the solvability of the RPT problem. Consider also the reference input $r(t)$ being a vector of step functions. Then, the reduced order measurement feedback control law of the form (6) with its gain matrices being given as in (46) solves the RPT problem for $\sum$ with the reference $r(t)$. □

We now ready to move on the design of our proposed servo system. We will design a servo system that meets the following design specifications:

1) The control input should not exceed ±2 V due to physical constraints on the actual VCM actuator.
2) The overshoot and undershoot of the step response should be kept less than 5% as the R/W head can start to read or write within ± 5% of the target.
3) The 5% settling time in the step response should be less than 2 ms (to beat the PID controller).
4) Sampling frequency in implementing the actual controller is 4 kHz, which is the sampling frequency currently used in most commercial disk drives.

From experience that we gained in designing PID controllers, we know that it is quite safe to ignore the resonance models of the VCM actuator if we are focusing on tracking performance. Thus, we will consider only a second-order model for the VCM actuator at this stage. We will then put the resonance modes back when we are to evaluate the performance of the overall design. Thus, we will use the following simplified model of the VCM actuator,

$$\dot{x} = \begin{bmatrix} 0 & 1 \\ 0 & 0 \end{bmatrix} x + \begin{bmatrix} 0 \\ 44\,296\,000 \end{bmatrix} u \tag{47}$$

and

$$y = h = [1 \;\; 0]x \tag{48}$$

in our design. It is simple to verify that the above system satisfies the solvability conditions for the RPT problem. The correspond-

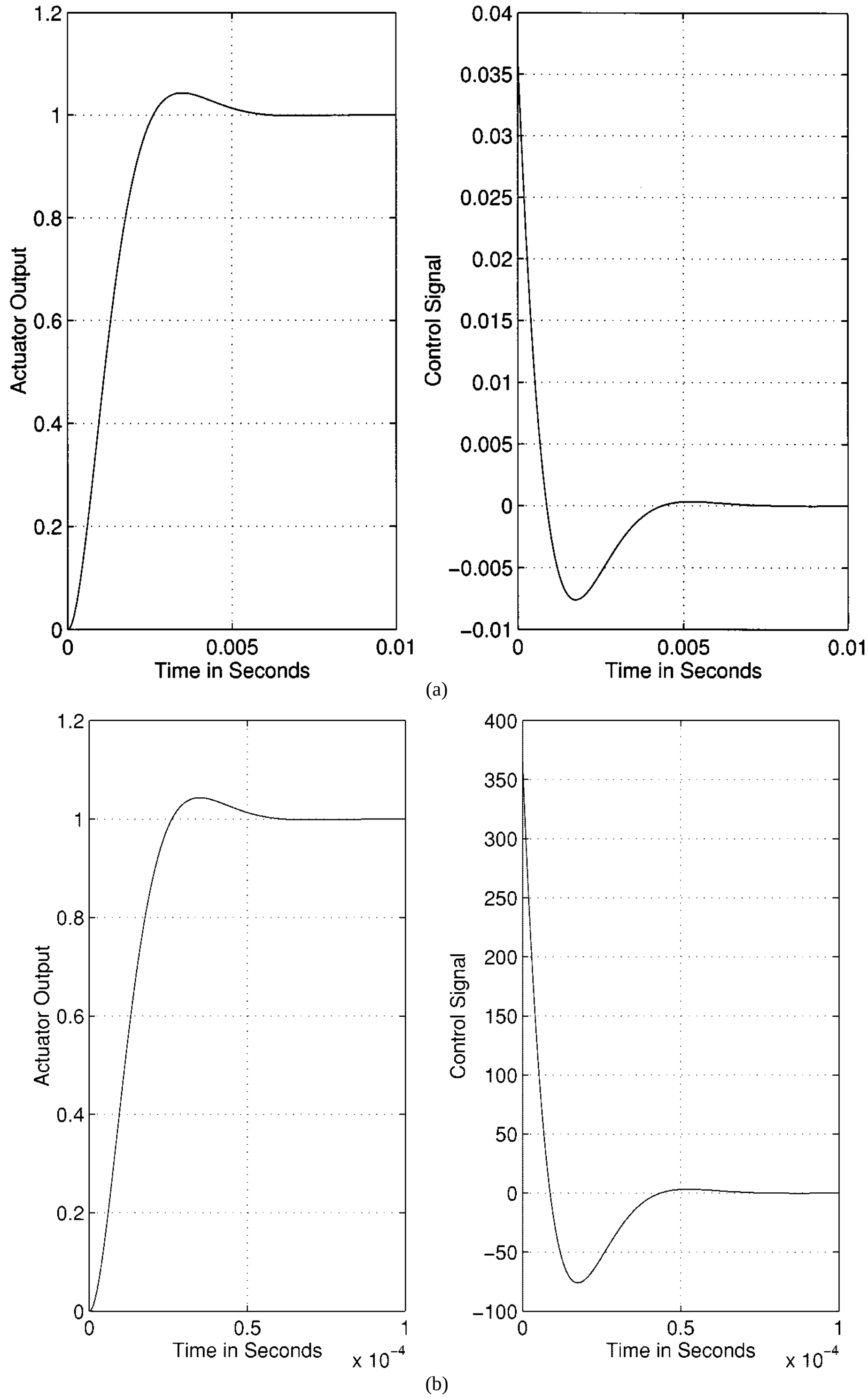

Fig. 3. Responses of the closed-loop systems with parameterized RPT controller. (a) $\varepsilon - 1$. (b) $\varepsilon = 0.01$.

ing auxiliary system in the format of (10) for the above plant can be expressed as

$$\left.\begin{aligned} \dot{\boldsymbol{x}} &= \begin{bmatrix} 0 & 0 & 0 \\ 0 & 0 & 1 \\ 0 & 0 & 0 \end{bmatrix} \boldsymbol{x} + \begin{bmatrix} 0 \\ 0 \\ 44\,296\,000 \end{bmatrix} u + \begin{bmatrix} 1 \\ 0 \\ 0 \end{bmatrix} \boldsymbol{w} \\ \boldsymbol{y} &= \begin{bmatrix} 1 & 0 & 0 \\ 0 & 1 & 0 \end{bmatrix} \boldsymbol{x} + \begin{bmatrix} 0 \\ 0 \end{bmatrix} \boldsymbol{w} \\ e &= [-1\ 1\ 0]\boldsymbol{x} + 0\boldsymbol{u} \end{aligned}\right\}. \tag{49}$$

Following the construction algorithm for the RPT controller, we obtained a parameterized first-order measurement feedback control law of the form (6) with

$$\left.\begin{aligned} A_{vv}(\varepsilon) &= -7800/\varepsilon \\ B_{vy}(\varepsilon) &= -4.842 \times 10^7/\varepsilon^2 \\ B_{vr}(\varepsilon) &= 1.62 \times 10^6/\varepsilon^2 \\ C_{vv}(\varepsilon) &= -4.063\,572 \times 10^{-5}/\varepsilon \\ D_{vy}(\varepsilon) &= -0.280\,386/\varepsilon^2 \\ D_{vr}(\varepsilon) &= 0.036\,572/\varepsilon^2 \end{aligned}\right\} \tag{50}$$

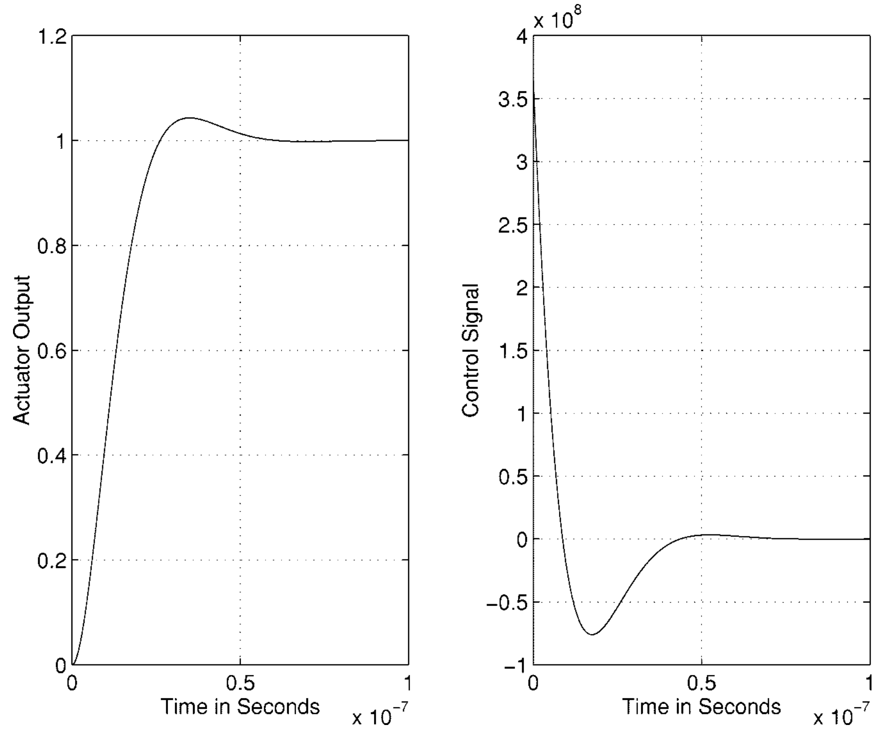

(c)

Fig. 3. *(Continued).* Responses of the closed-loop systems with parmeterized RPT controller. (c) $\varepsilon = 10^{-5}$.

Results in Fig. 3 are obtained using a Matlab package. They clearly show that the RPT problem is solved as we tune the tuning parameter ε to be smaller and smaller. Unfortunately, due to the constraints of the physical system, i.e., the limits in control inputs and sampling rates, as well as resonance modes, it is impossible to implement a controller that will track the reference in zero time. We would thus have to make some compromises in the track following speed because of these limitations. After several trials, we found that the controller parameters of (50) with $\varepsilon = 0.9$ would give us a satisfactory performance. We then discretize it using a bilinear transformation with a sampling frequency of 4 kHz. Note that it was shown in Chen and Weller [3] that the bilinear transformation does not introduce additional nonminimum phase invariant zeros and it preserves the invertibility structure of the system. The discretized controller is given by

$$x_v(k+1) = -0.04x_v(k) + 15\,178.933r(k) - 453\,681.43y(k)$$
$$u(k) = -3.4267\times 10^{-7}x_v(k) + 0.039\,73r(k) - 0.184\,21y(k).$$

Fig. 4 shows that the step response of the overall system comprising the fourth-order model of the VCM actuator (we now put the resonance modes back into the VCM actuator model) and the discretized RPT controller, meets the design specifications. In actual hard disk drive manufacturing, the resonant frequency ω_n of the VCM actuator for the same batch of drives might vary from one to the other [see (4)]. A common practice in the disk drive industry is to add some notch filters in the servo system to attenuate these resonant peaks as much as possible. Surprisingly, our RPT controller is capable of withstanding the variation of resonance frequencies as well. Fig. 5 shows the step responses of the closed-loop systems of our RPT controller and the VCM model with two different resonant frequencies: one is 1.125 kHz, which is $\beta = 75\%$ of the nominal value, and the other is 2.25 kHz, which is $\beta = 150\%$ of the nominal resonant frequency. The results show that the RPT controller is very robust with respect to the change of resonant frequency in the actuator.

Although we do not consider the effects of run-out disturbances in our problem formulation, it turns out that our simple first order controller is capable of rejecting the first few modes of the run-out disturbances, which are mainly due to the imperfectness of the data tracks and the spindle motor speeds, and commonly have frequencies at the multiples of about 55 Hz. We simulate these run-out effects by injecting a sinusoidal signal into the measurement output, i.e., the new measurement output is the sum of the actuator output and the run-out disturbance. Fig. 6 shows the simulation result of the output response of the overall servo system comprising the fourth-order model of the VCM actuator model and the discretized RPT controller with a fictitious run-out disturbance injection $\tilde{w}(t) = 0.5 + 0.1\cos(110\pi t) + 0.05\sin(220\pi t)$ and a zero reference $r(t)$. The result shows that the effects of such a disturbance to the overall response are minimal. A more comprehensive test on run-out disturbances, i.e., the position error signal (PES) test on the actual system will be presented in the next section.

IV. Implementation Results

In this section, we present the actual implementation results of our design and their comparison with those of a PID controller. Two major tests are presented: one is the track following of the closed-loop systems and the other is the position error signal (PES) test, which is considered to be a major factor in design hard disk drive servo systems. Our controller was implemented on an open hard disk drive with a TMS320 digital signal

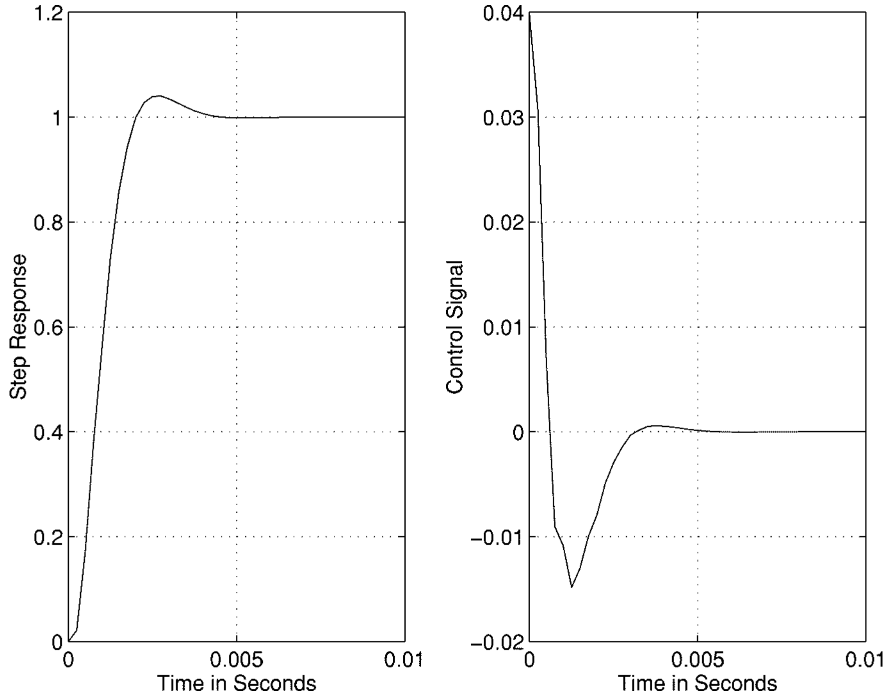

Fig. 4. Step response of the closed-loop system with the discretized RPT controller.

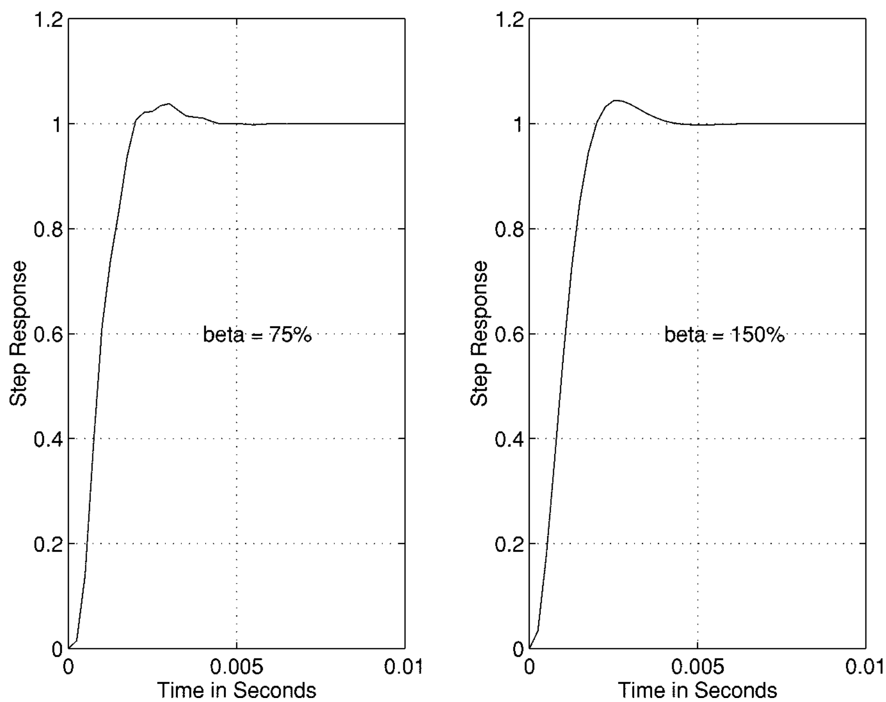

Fig. 5. Step responses of the closed-loop system with different resonant frequencies.

processor (DSP) and a sampling rate of 4 kHz. Closed-loop actuation tests were performed using a laser doppler vibrometer (LDV) to measure the R/W head position. The resolution used for LDV was 1 μm/V. This displacement output is then fed into the DSP, which would then generate the necessary control signal to the VCM actuator. A digital signal analyzer (DSA) was used to assist in obtaining the frequency response of the overall control system. It can inject a swept sinusoidal reference signal, then read the output displacement from the LDV and calculate the frequency Bode plot using this information. Altogether, two sets of experiment were performed, one using the RPT controller and the other using a PID controller reported in Goh [7].

A. Track Following Test

The solid-line curve in Fig. 7 shows the experimental step response of the RPT controller. In this figure, the response of the RPT controller is shown together with that of a PID controller

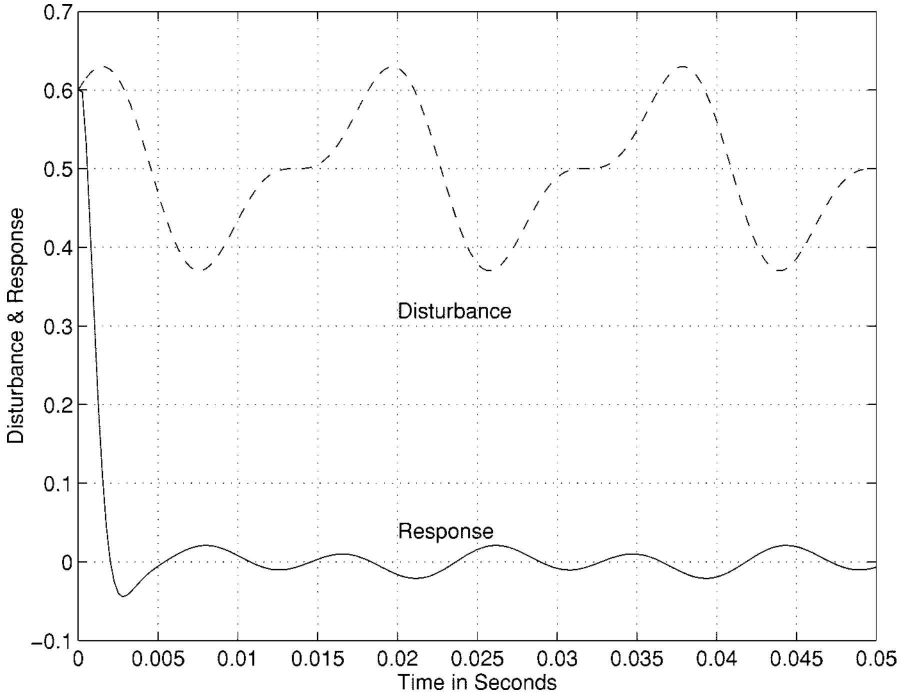

Fig. 6. Output response of the closed-loop system due to a run-out disturbance.

of Goh [7] as a comparison. Note that the actual response of the closed-loop system with the RPT controller is slightly faster and its overshoot is slightly larger (about 7%) compared to the simulation results given in the previous section. The 5% settling time is about 1.6 ms, which surely meets the design specifications. Fig. 8 shows the experimental closed-loop Bode plot. It shows that the system has a closed-loop bandwidth of about 500 Hz. At the roll-off frequency, there is no discernible resonance peak.

The dotted-line curve in Fig. 7 shows the step response of the PID controller of Goh [7] (again using a 4 kHz sampling rate). The PID controller had a usual structure and was tuned such that it could have fast time response. It is given by

$$u = \frac{0.13z^2 - 0.23z + 0.10}{z^2 - 1.25z + 0.25}(r - y). \quad (51)$$

Unfortunately, the overshoot of the controller is rather high, about 50% and this is a result of trading improved settling time at the expense of higher overshoot. To achieve a settling time of 4–5 ms, it is necessary to tune the PID controller such that the overshoot is significant. Fig. 9 shows the experimental closed-loop Bode plot of the PID controller. The closed-loop bandwidth of this servo system is also about 500 Hz, with a slight peak of about 7 dB at the roll-off frequency. This resonance peak would result in additional tracking errors close to the bandwidth frequency.

Remark 1: We believe that the shortcoming of the PID control is mainly due to its structure, i.e., it only feeds in the error signal, $y - r$, instead of feeding in both y and r independently. On the other hand, the RPT control scheme can be regarded as a structure with two degrees of freedom, which feeds in both y and r. The PID control structure might be simple as most of researchers and engineers have claimed. However, our RPT controller is even simpler, i.e., the RPT controller is of the first order and the PID controller is of the second order. The main reason that the RPT control outperforms the PID is: In the RPT structure, all available information associated with the system is fully utilized, while in the PID control, only partial information is used. □

Unfortunately, we could not compare our results with those of other methods mentioned in the introduction. Most of references we found in the literature contained only simulation results in this regard. Some of implementation results we found were, however, very different in nature. For example, Hanselmann and Engelke of [8] reported an implementation result of a disk drive servo system design using the LQG approach with a sampling frequency of 34 kHz. The overall step response of [8] with a higher order LQG controller and higher sampling frequency is worse than that of ours.

B. *Position Error Signal Test*

The disturbances in a real hard disk drive are usually considered as a lumped disturbance at the plant output, also known as run-outs. Repeatable run-outs (RROs) and nonrepeatable run-outs (NRROs) are the major sources of track following errors. RRO is caused by the rotation of the spindle motor and consists of frequencies that are multiples of the spindle frequency. NRRO can be perceived as coming from three main sources: vibration shocks, mechanical disturbance, and electrical noise. Static force due to flex cable bias, pivot-bearing friction and windage are all components of the vibration shock disturbance. Mechanical disturbances include spindle motor variations, disk flutter, and slider vibrations. Electrical noises include quantization errors, media noise, servo demodulator noise, and power amplifier noise. NRRO are usually random and unpredictable by nature, unlike RROs. They are also of a lower magnitude (see, e.g., [6]). A perfect servo system of hard disk drives should reject both the RRO and NRRO.

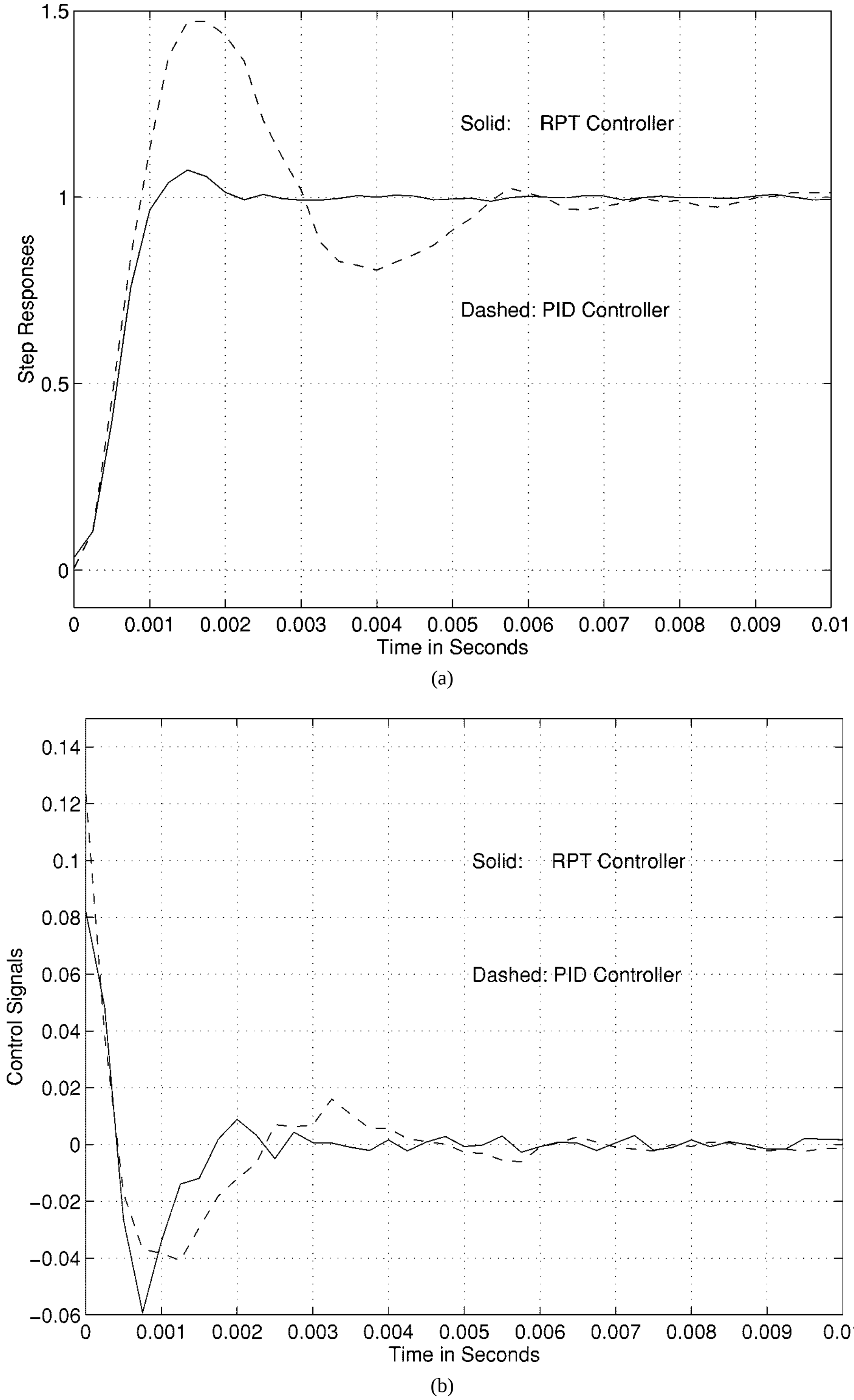

Fig. 7. Implementation result: Step responses of closed-loop systems with RPT and PID controllers.

In our experiment, we have simplified the system somewhat by removing many sources of disturbances, especially that of the spinning magnetic disk. Therefore, we have to actually add the run-outs and other disturbances into the system manually. Based on previous experiments, we know that the run-outs in real disk drives is mainly composed of the RRO, which is basically sinusoidal with a frequency of about 55 Hz, equivalent to the spin rate of the spindle motor. By manually adding this "noise" to the output while keeping the reference signal to zero, we can then read off the subsequent position signal as the expected PES in the presence of run-outs. In disk drive applications, the variations of the R/W head from the center of track during track following, which can be directly read off as the position error signal (PES), is very important. Track following servo systems have to ensure that the PES is kept to a minimum. Having deviations that are above the tolerance of the disk drive would result in too many read or write errors, making the disk drive unusable. A suitable measure is the standard deviation of

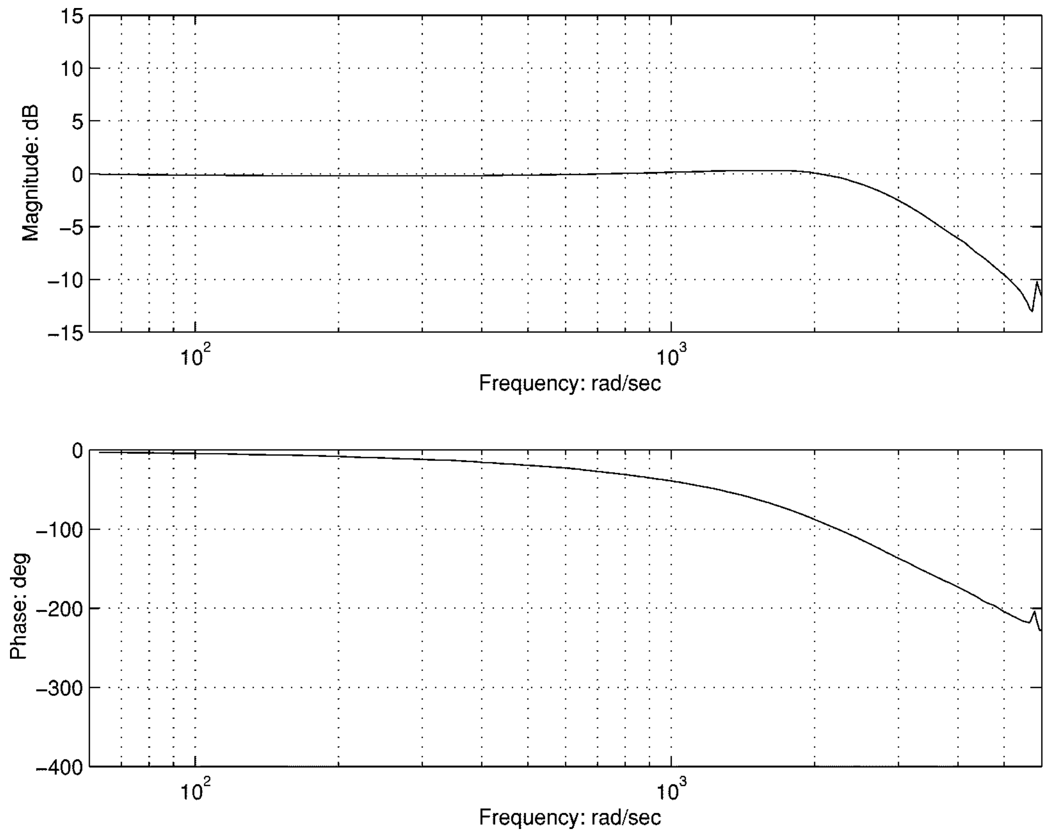

Fig. 8. Implementation result: Closed-loop frequency response of system with RPT controller.

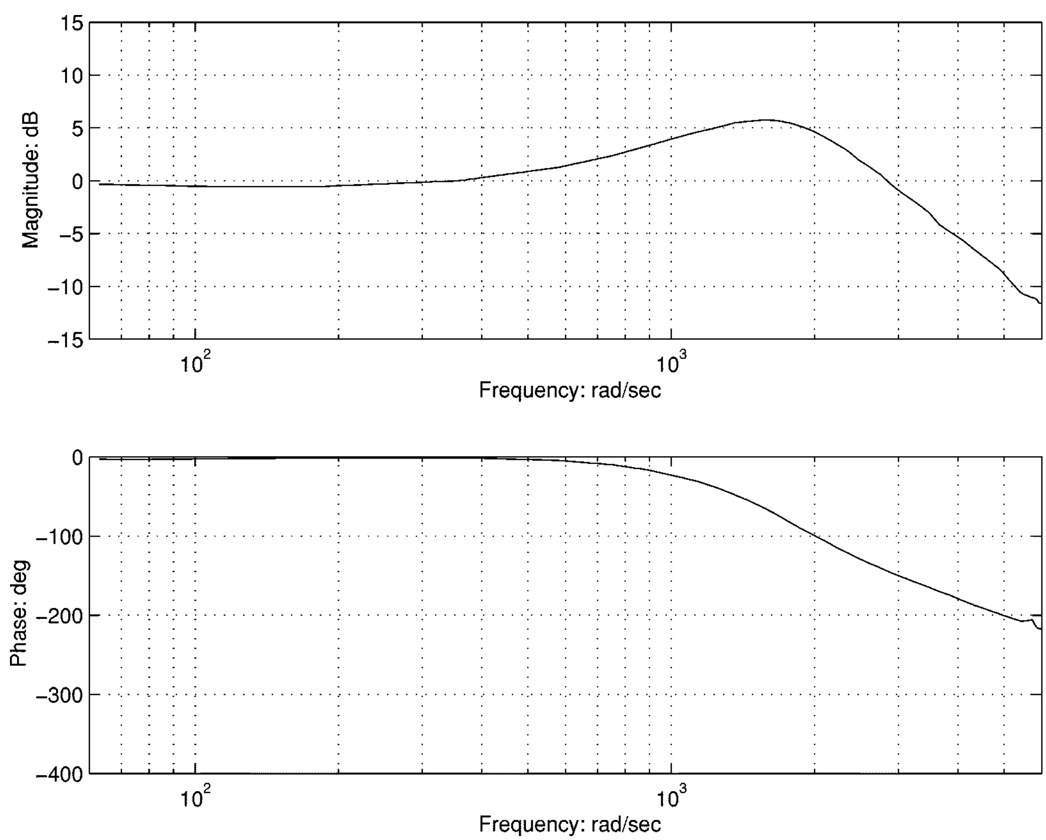

Fig. 9. Implementation result: Closed-loop frequency response of system with PID controller.

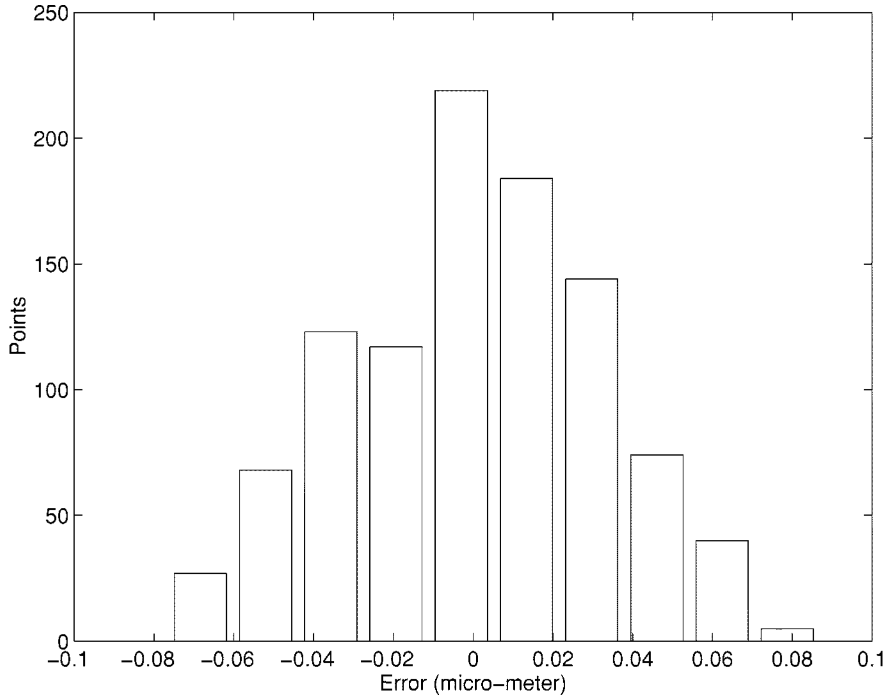

Fig. 10. Implementation result: Histogram of the PES test with the RPT controller.

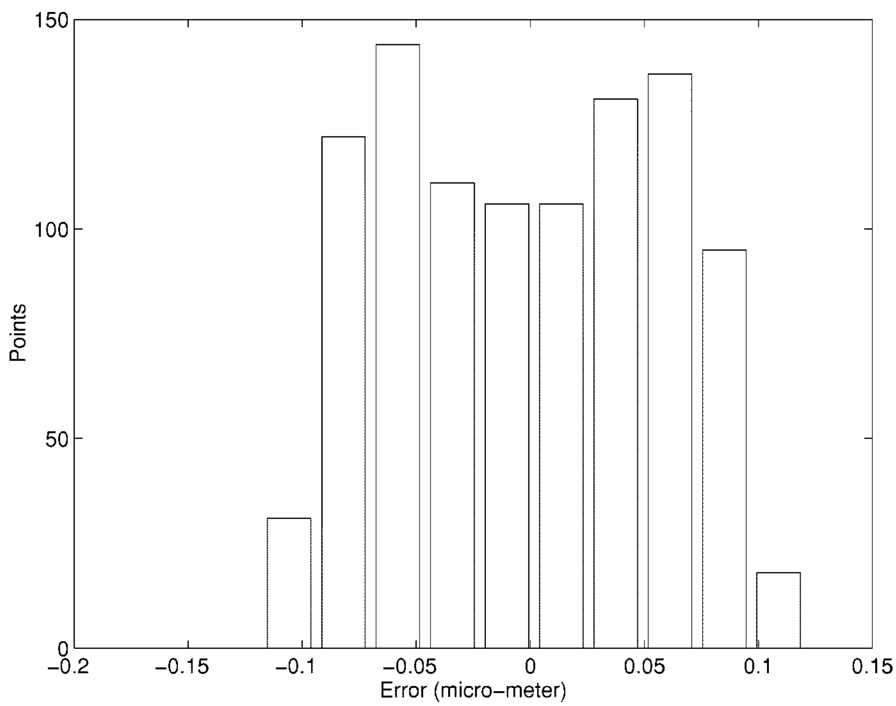

Fig. 11. Implementation result: Histogram of the PES test with the PID controller.

the readings, σ. A useful guideline is to make the 3σ value less than 5% of the track width, which is about 0.1 μm for a track density of 10–15 kTPI (kilo tracks per inch).

Figs. 10 and 11 show the tracking errors of robust and perfect tracking controller and PID controller, respectively, under the disturbance of the run-outs. The 3σ value is about 0.095 μm for the RPT controller, and about 0.175 μm for the PID controller. Again, the RPT controller does better than the PID one in the PES test.

V. Concluding Remarks

A so-called robust and perfect tracking controller design for a hard disk drive servo system has been reported in this paper. The RPT controller has a much better performance in track following as well as in the PES tests compared to those of the PID controller as well as other controllers. The RPT controller has very minimal overshoot and undershoot and much faster settling time.

The RPT controller utilized is first order. This is one order lower in comparison with the PID controller and would allow for quicker execution of the DSP codes during implementation. This would be an important consideration when the sampling rate of the disk drive servo is pushed higher to meet the increasing demands on the servo performance. The current results can be further improved if we used a better VCM actuator and arm assembly, with a higher resonance frequency. The control input limit has not been reached and theoretically, we should be able to tune the controller to achieve even faster settling time and higher servo bandwidth. This will be a subject of our future work.

REFERENCES

[1] B. M. Chen, H_∞ *Control and Its Applications*. New York: Springer-Verlag, 1998.

[2] ——, "Linear Systems and Control Toolbox," Dept. Elect. Eng., Nat. Univ. Singapore, Tech. Rep., 1997.

[3] B. M. Chen and S. R. Weller, "Mappings of the finite and infinite zero structures and invertibility structures of general linear multivariable systems under the bilinear transformation," *Automatica*, vol. 34, no. 1, pp. 111–124, 1998.

[4] B. M. Chen, T. H. Lee, C. C. Hang, Y. Guo, and S. Weerasooriya, "An H_∞ almost disturbance decoupling robust controller design for a piezoelectric bimorph actuator with hysteresis," *IEEE Trans. Contr. Syst. Technol.*, vol. 7, pp. 160–174, 1999.

[5] P. Eykhoff, *System Identification—Parameter and State Estimation*. New York: Wiley, 1981.

[6] G. F. Franklin, J. D. Powell, and M. L. Workman, *Digital Control of Dynamic Systems*. New York: Addison-Wesley, 1990.

[7] T. B. Goh, "Development of a Dual Actuator Controller in Hard Disk Drives," M.S. thesis, Dep. Elect. Eng., Nat. Univ. Singapore, 1999.

[8] H. Hanselmann and A. Engelke, "LQG-control of a highly resonant disk drive head positioning actuator," *IEEE Trans. Ind. Electron.*, vol. 35, pp. 100–104, 1988.

[9] Z. Lin, "The Implementation of Special Coordinate Basis for Linear Multivariable Systems in Matlab," Washington State Univ. Tech. Rep. ECE0100, Pullman, WA, 1989.

[10] K. Liu, B. M. Chen, and Z. Lin, "On the problem of robust and perfect tracking for linear systems with external disturbances," in *Proc. Amer. Contr. Conf.*, Chicago, IL, June 2000, pp. 887–891.

[11] J. McCormick and R. Horowitz, "A direct adaptive control scheme for disk file servos," in *Proc. 1993 Amer. Contr. Conf.*, San Francisco, CA, 1993, pp. 346–351.

[12] A. Saberi and P. Sannuti, "Squaring down of nonstrictly proper systems," *Int. J. Contr.*, vol. 51, no. 3, pp. 621–629, 1990.

[13] P. Sannuti and A. Saberi, "A special coordinate basis of multivariable linear systems—Finite and infinite zero structure, squaring down and decoupling," *Int. J. Contr.*, vol. 45, no. 5, pp. 1655–1704, 1987.

[14] L. Wang, L. Yuan, B. M. Chen, and T. H. Lee, "Modeling and control of a dual actuator servo system for hard disk drives," in *Proc. 1998 Int. Conf. Mechatron. Technol.*, Hsinchu, Taiwan. R.O.C., 1998, pp. 533–538.

[15] S. Weerasooriya, "The Basic Servo Problem," Data Storage Inst., Nat. Univ. Singapore, Singapore, Tech. Rep., 1996.

[16] S. Weerasooriya and D. T. Phan, "Discrete-time LQG/LTR design and modeling of a disk drive actuator tracking servo system," *IEEE Trans. Ind. Electron.*, vol. 42, pp. 240–247, 1995.

Teck B. Goh was born in Singapore on October 1, 1972. He received the Bachelor of Engineering and Master of Engineering degrees in electrical engineering from the National University of Singapore, in 1997 and 1999, respectively.

He was a Design Engineer with Lucus Origin Private Limited, Singapore, from 1999 to 2000. Since March 2000, he has been with Philips Electronics Singapore Private Limited, where he is currently a Software Engineer.

Zhongming Li was born in Heilongjiang, China, on January 8, 1971. He received the B.S. degree in 1992 and the M.E. degree in 1995, both in electrical engineering, from the Harbin Institute of Technology, Harbin, China. Since 1998, he has been pursuing the Ph.D. degree at the Department of Electrical Engineering, the National University of Singapore.

From 1995 to 1997, he was an Electrical Engineer with the China National Offshore Oilfield Corporation, China. His current research interests include control applications and design of computer hard disk drive servo systems.

Ben M. Chen (S'89–M'92) was born in Fuqing, Fujian, China, on November 25, 1963. He received the B.S. degree in mathematics and computer science from Amoy University, Xiamen, China, in 1983, M.S. degree in electrical engineering from Gonzaga University, Spokane, WA, in 1988, and Ph.D. degree in electrical and computer engineering from Washington State University, Pullman, in 1991.

He was a Software Engineer from 1983 to 1986 in the South-China Computer Corporation, China, and was a Postdoctoral Associate from 1991 to 1992 with Washington State University. He was with the Department of Electrical Engineering, State University of New York, Stony Brook, from 1992 to 1993, as an Assistant Professor. Since August 1993, he has been with Electrical Engineering Department, the National University of Singapore, where he is currently an Associate Professor. His current research interests are in linear control and system theory, control applications, development of internet-based virtual laboratories and internet security systems. He is the author of the books *Robust and* H_∞ *Control* (New York: Springer-Verlag, 2000), and H_∞ *Control and Its Applications* (New York: Springer-Verlag, 1998), and coauthor of the books *Loop Transfer Recovery: Analysis and Design* (New York: Springer-Verlag, 1993), *H2 Optimal Control* (Englewood Cliffs, NJ: Prentice-Hall, 1995), and *Basic Circuit Analysis* (Singapore: Prentice-Hall Asia, first ed., 1996; second ed., 1998).

Dr. Chen was an Associate Editor in 1997–1998 on the Conference Editorial Board of IEEE Control Systems Society. He currently serves as an Associate Editor of IEEE TRANSACTIONS ON AUTOMATIC CONTROL.

Tong Heng Lee (M'88) received the B.A. degree with First Class Honors in the engineering tripos from Cambridge University, Cambridge, U.K., and the Ph.D. degree from Yale University, New Haven, CT, in 1980 and 1987, respectively.

He is a Professor in the Department of Electrical Engineering at the National University of Singapore. He is also currently Head of the Control Engineering Division in this Department, and the Vice-Dean (Research) in the Faculty of Engineering. His research interests include adaptive systems, knowledge-based control, and intelligent mechatronics. He has published extensively in these areas, and currently holds Associate Editor appointments in *Automatica*, *Control Engineering Practice*, the *International Journal of Systems Science*, and *Mechatronics*.

Dr. Lee was a recipient of the Cambridge University Charles Baker Prize in Engineering. He is an Associate Editor of the IEEE TRANSACTIONS ON SYSTEMS, MAN, AND CYBERNETICS.

Tony C. Huang (S'90–M'97) was born in Taiwan in 1965. He received the B.S., M.S., and Ph.D. in electrical engineering all from the University of Washington, Seattle, in 1987, 1989, and 1995, respectively.

He joined the Servo Electronics group of Data Storage Institute, Singapore, in 1995. In 1997, he was promoted to Manager of the Servo Electronics group. In 1999, he joined Seagate Technology Colorado. His current research interests include real-time control systems and evaluation tools and servo systems for data storage devices.